Electronic Supplementary Material (ESI) for New Journal of Chemistry.

The effect of π-linker bulky on photophysical properties of 2-phenylfuro[2,3-b]quinoxaline-based FQ-π-FQ typed compounds

ChuanMing Wu†, MingXin Wu †, BoHua Zhang, MeiTing Luo, Dongdong Wang*, Yong Wu, GuoXin Yang, Lei Gou, and Zhaoxin Wu

Section one: Synthesis and characterization

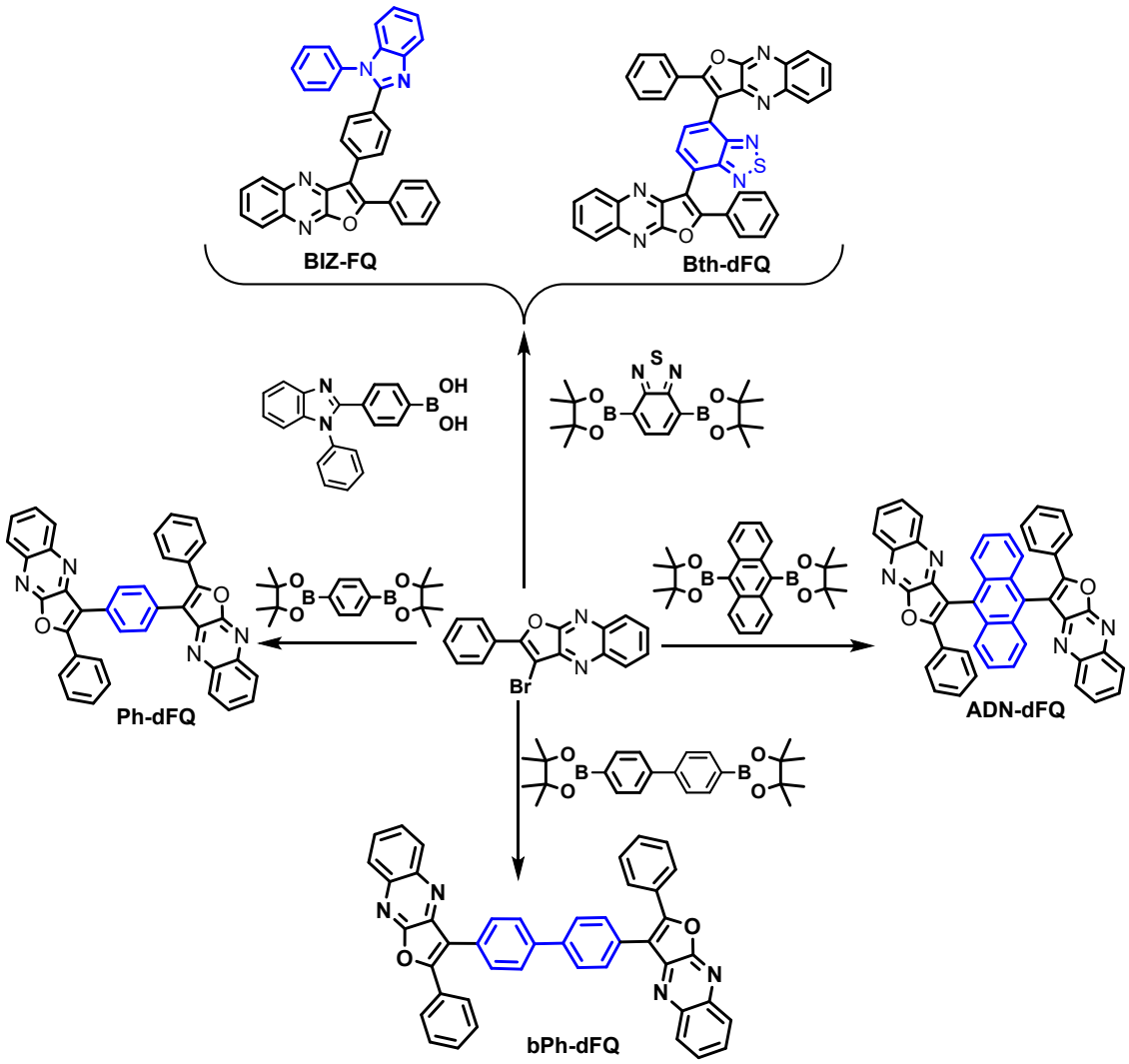

Scheme 1 the synthesis routes of five compounds.

General procedure for synthesizing of Ph-dFQ, bPh-dFQ, ADN-dFQ, and Bth-dFQ.

3-bromo-2-phenylfuro[2,3-b]quinoxaline (2.2 eq), diborate compounds (1 eq), Cs_2CO_3(6.0 eq) and $Pd(PPh_3)_4$ (10% eq) were added to 40mL anhydrous toluene. Then the reaction mixture was stirred at 100°C under a nitrogen atmosphere until TLC revealed complete conversion of the starting material. The mixture was filtered and washed with DCM and THF, respectively. The compound could not be dissolved in most of common solvents, and so it was purified by sublimating technology.

Ph-dFQ (0.5g, 68%): 3-bromo-2-phenylfuro[2,3-b]quinoxaline (0.91g, 2.8mmol), 1,4-bis(4,4,5,5-tetramethyl-1,3,2-dioxaborolan-2-yl)benzene(0.424g, 1.3mmol), Cs_2CO_3(2.77g, 7.65 mmol) and $Pd(PPh_3)_4$ (0.065 mmol). ^{1}HNMR (800 MHz, Chloroform-d) δ (ppm) 8.31 (d, J = 7.0 Hz, 2H), 8.18 (d, J

= 7.0 Hz, 2H), 8.00 -7.97 (m, 4H), 7.95 (s, 4H),7.83 -7.74 (m, 4H), 7.52 - 7.45 (m, 5H). HRMS(ESI) m/z: $[M+H]^+$: calculated for $C_{38}H_{22}N_4O_2$ 567.18155; found 567.18022. Element Analysis (%): calculated for $C_{38}H_{22}N_4O_2$: C,80.55; H,3.914; O,5.65; N, 9.888; found C, 80.45; H, 3.882; O, 5.760; N, 9.840.

bPh-dFQ (0.45g, 70%): 3-bromo-2-phenylfuro[2,3-b]quinoxaline(0.715g, 2.2mmol), 4,4'-bis(4,4,5,5-tetramethyl-1,3,2-dioxaborolan-2-yl)-1,1'-biphenyl (0.911g, 1mmol), Cs_2CO_3(2.4g, 6.4mmol) and $Pd(PPh_3)_4$(0.12g, 0.1mmol). ^{1}H NMR (800 MHz, Chloroform-d) δ (ppm) 8.31 (d, J = 7.7 Hz, 2H), 8.19 (d, J = 7.7 Hz, 2H), 7.95 (d, J = 7.4 Hz, 4H), 7.88 (s, 8H), 7.79 - 7.77 (m, 4H), 7.49 - 7.47 (m, 6H). HRMS(ESI) m/z: [M+H]+:calculated for C44H26N4O2 643.21285; found 643.21203. Element Analysis (%): calculated for $C_{44}H_{26}N_4O_2$: C,82.05; N,8.505; O,4.857; H, 4.590; found C,81.85; H,4.008; O, 5.023; N,8.770.

ADN-dFQ (0.18g, 31%): 3-bromo-2-phenylfuro[2,3-b]quinoxaline(0.78g, 2.5mmol), 9,10-bis(4,4,5,5-tetramethyl-1,3,2-dioxaborolan-2-yl)anthracene (0.5g, 1.16mmol), Cs_2CO_3(2.53g, 6.9mmol) and $Pd(PPh_3)_4$(0.14g, 0.13mmol). ^{1}H NMR (400 MHz, $CDCl_3$): δ (ppm) 8.23-8.25 (d, *J* = 8.0 Hz, 2H), 8.12-8.14 (d, *J* = 8.0 Hz, 1H), 8.02-8.05 (d, *J* = 12 Hz, 1H), 7.86-7.90 (m, 4H), 7.76 - 7.80 (m, 2H), 7.67 - 7.72 (m, 4H), 7.57 - 7.59 (m, 4H), 7.29-7.36 (m, 8H), 7.18-7.22 (t, 2H). HRMS(ESI) m/z: $[M+H]^+$: calculated for $C_{46}H_{26}N_4O_2$ 667.21285; found 667.21314. Element Analysis (%): calculated for $C_{46}H_{26}N_4O_2$: C,82.87; H,3.931; O,4.799; N,8.403, found C,83.07; H,3.900; O,4.856; N,8.300.

Bth-dFQ (0.22g, 30%): 3-bromo-2-phenylfuro[2,3-b]quinoxaline (0.76g, 2.55mmol), 4,7-bis(4,4,5,5-tetramethyl-1,3,2-dioxaborolan-2-yl)benzo[c][1,2,5]thiadiazole (0.453g, 1.17mmol), Cs_2CO_3 (2.5g, 6.9 mmol) and $Pd(PPh_3)_4$ (0.13g, 0.117mmol). ^{1}HNMR (600 MHz, $CDCl_3$): δ (ppm) 8.30 (s, 2H), 8.20-8.22 (d, J=12Hz, 4H), 7.74-7.81 (m, 8H), 7.43-7.46 (t, 2H), 7.36-7.38 (t, 4H); ^{13}CNMR (600 MHz, $CDCl_3$): δ (ppm) 155.5, 149.0, 139.4, 137.6, 134.5, 127.2, 126.2, 124.5,123.7,119.5,107.6; HRMS(ESI) m/z: $[M+H]^+$:calculated for $C_{38}H_{20}N_6O_2S$ 625.14412; found 625.14535. Element Analysis (%): calculated for $C_{38}H_{20}N_6O_2S$: C,73.06; H,3.23; O,5.12; N,13.45; S,5.13; found C,72.62; H,3.156; O,5.133; N,13.60; S,5.194.

BIZ-FQ (0.24 g, 23%): 3-bromo-2-phenylfuro[2,3-b]quinoxaline(0.65g, 2 mmol), (4-(1-phenyl-3a,7a-dihydro-1H-benzo[d]imidazol-2-yl)phenyl)boronic acid (0.785g, 2.5mmol), K_2CO_3(0.68g, 5mmol) and $Pd(PPh_3)_4$(0.12g, 0.1mmol) were added to 100 ml dioxane/H_2O (4:1) mixed solvent. Then the reaction mixture was stirred at 120℃ under a nitrogen atmosphere until TLC revealed complete conversion of

the starting material. The mixture was then cooled, poured into water and filtered. The residue was resolved with 100 ml CH_2Cl_2 and purified by silica gel column chromatography (CH_2Cl_2 / petroleum ether) to give the corresponding product. ^{1}HNMR (400 MHz, Chloroform-d) δ (ppm) 8.25 -8.17 (m, 1H), 8.17 -8.09 (m, 1H), 7.93 (d, J = 8.0 Hz, 1H), 7.85 - 7.78 (m, 2H), 7.78 - 7.69 (m, 6H), 7.60 -7.50 (m, 3H), 7.45 -7.35 (m, 6H), 7.32 -7.25 (m, 2H). HRMS(ESI) m/z: $[M]^+$: calculated for $C_{35}H_{22}N_4O$ 516.19446; found 516.19103. Element Analysis (%): calculated for $C_{35}H_{22}N_4O$: C,81.69; H,4.31; O,3.11; N,10.89; found C,81.44; H,4.650; O,3.243; N,10.96.

Section two: Measurements and device fabrication

TGA-DSC measurements were carried out on a Shimadzu DTG-60 instrument from room temperature to 500 °C under dry nitrogen flow with a heating rate of 10 °C/min. UV-visible spectra of solution were recorded on Hitchi 3010 spectrometers. The steady state and transient fluorescence spectra were measured on FLS 980 fluorescent spectrometer, and fluorescence quantum yields (PLQY) was measured via using the integrating sphere in combination with FLS980 spectrofluorometer.

Device fabrication and characterization. All the organic layers were successively deposited by means of vacuum deposition onto the ITO-coated glass substrates, which were previously etched, patterned, and washed with detergent, deionized water, acetone, and ethanol in turn. For the doped layer, the dopant and host materials were co-evaporated and the doping concentrations was controlled by deposition rates. The electroluminescence spectra and CIE coordinates of the devices were measured by a spectrometer (PR655) and the current-voltage-luminescence characteristics were analyzed using Keithley 2400 source meter with PR655.

Section three: supplementary tables and Figures

Table 1. Fluorescence emissions in toluene of the studied compounds calculated by the TD-DFT method

	Electronic transition	**λ (nm)**	***f***	**Excitation energies(eV)**	**Configuration**
Ph-dFQ	$S_1 \rightarrow S_0$	$475/475^{Exp}$	0.3629	2.6092	H→L(97%)
	$S_2 \rightarrow S_0$	433	0.1661	2.8632	H→L+1(97%)
	$S_3 \rightarrow S_0$	353	0.5066	3.5103	H-1→L(47%)
					H→L+2(43%)
bPh-dFQ	$S_1 \rightarrow S_0$	$452/473^{Exp}$	0.4915	2.7439	H→L(92%)
	$S_2 \rightarrow S_0$	437	0.2385	2.8373	H→L+1(90%)
	$S_3 \rightarrow S_0$	361	1.1457	3.4371	H→L+2(65%)
					H-1→L+1(26%)
Bth-dFQ	$S_1 \rightarrow S_0$	$504/498^{Exp}$	0.3166	2.4606	H→L(98%)

	$S_2 \rightarrow S_0$	401.83	0.2208	3.0855	H→L+1(94%)
	$S_3 \rightarrow S_0$	400.49	0.3005	3.0958	H→L+2(93%)
AND-dFQ	$S_1 \rightarrow S_0$	498/507^{Exp}	0.0949	2.49	H→L(99%)
	$S_2 \rightarrow S_0$	486	0.0102	2.55	H→L+1(99%)
	$S_3 \rightarrow S_0$	429/440^{Exp}	0.3025	2.89	H→L+2(99%)
BIZ-FQ	$S_1 \rightarrow S_0$	470/471^{Exp}	0.3237	2.6359	H→L(96%)
	$S_2 \rightarrow S_0$	364	1.0970	3.4065	H→L+1(84%)
					H-1→L (10%)
	$S_3 \rightarrow S_0$	349	0.3238	3.5512	H-1→L(73%)
					H→L+1(12%)
					H-2→L(8%)

*exp indicated experimental value.

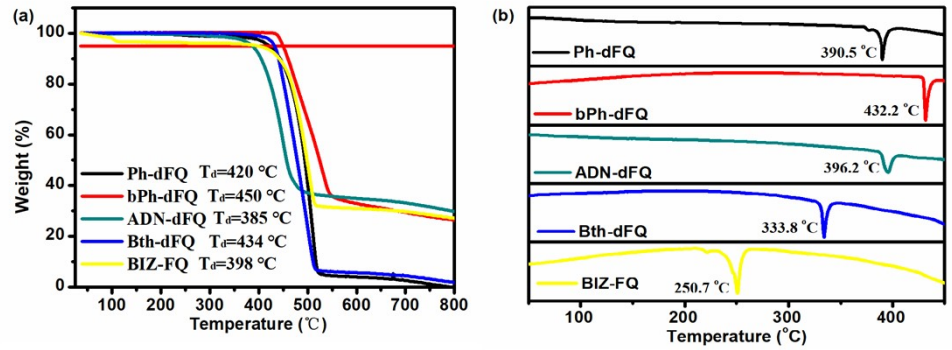

Figure S1 The thermogravimetric analysis and differential scanning calorimetry of five compounds

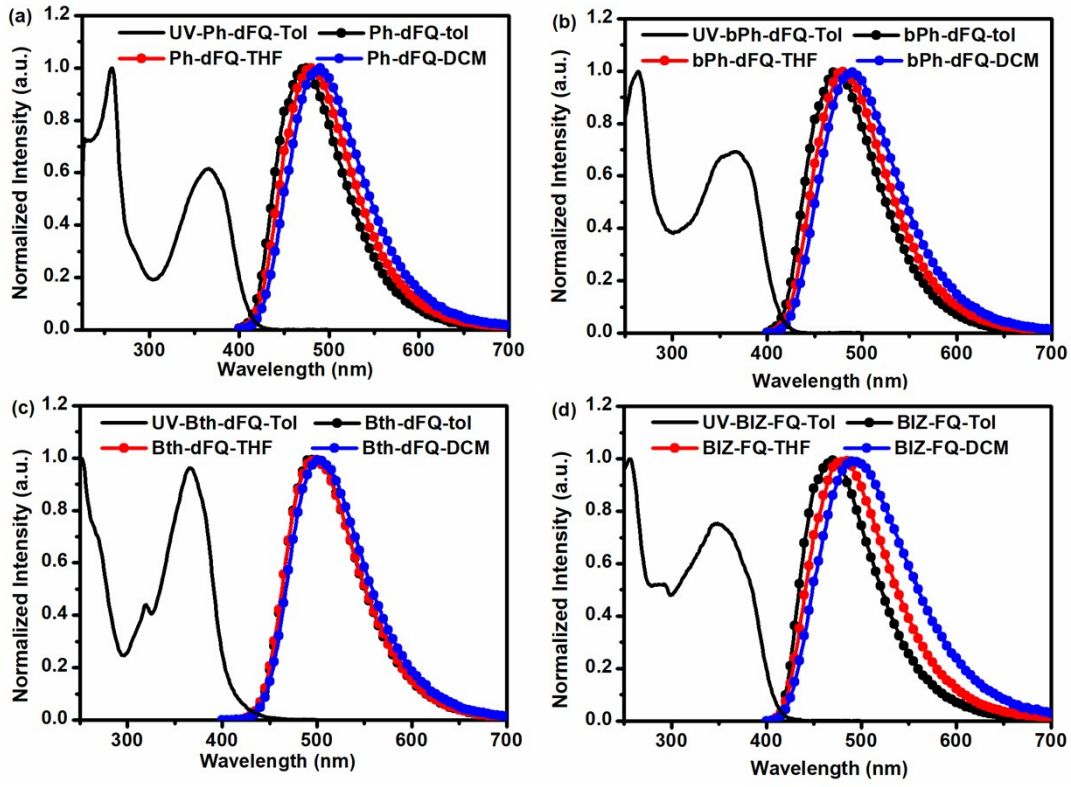

Figure S2 The PL spectra of four compounds Ph-dFQ, bPh-dFQ, ADN-dFQ and Bth-dFQ in different solvents, TOL, THF and DCM.

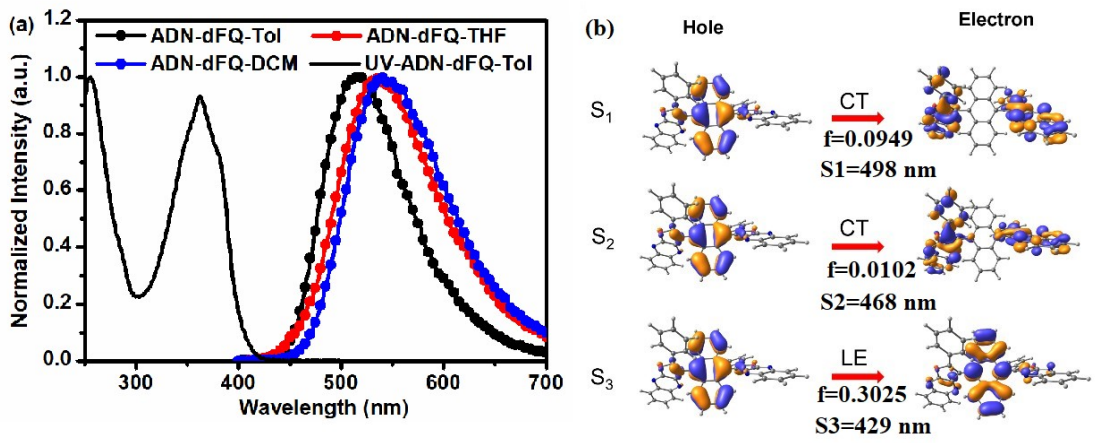

Figure S3. (a)The PL spectra of ADN-dFQ in solvents, TOL, THF and DCM; (b) natural transition orbitals and transition character of the key orbitals, S_1, S_2 and S_3, of AND-dFQ.

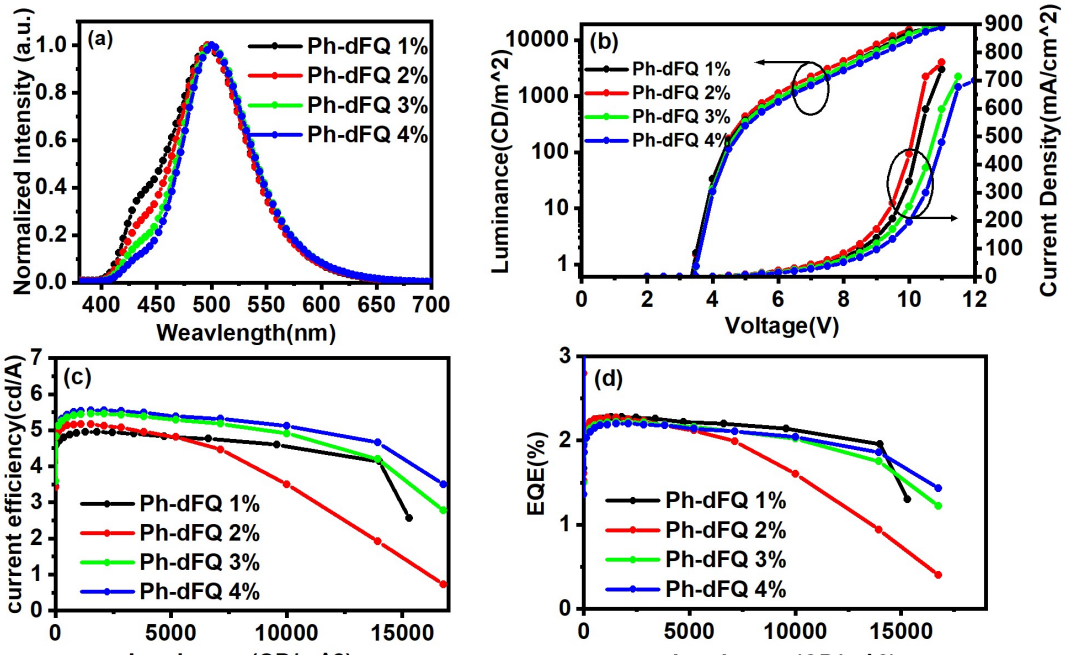

Figure S4. The EL performances of devices for compound Ph-dFQ as dopant concentration changed from 1% to 4%; (a) the EL spectrums at 8V for all the devices; (b) the current density–voltage-luminance (J-V-L) curves; (c) and (d) for the current efficiency and EQE vs luminance curves, respectively.

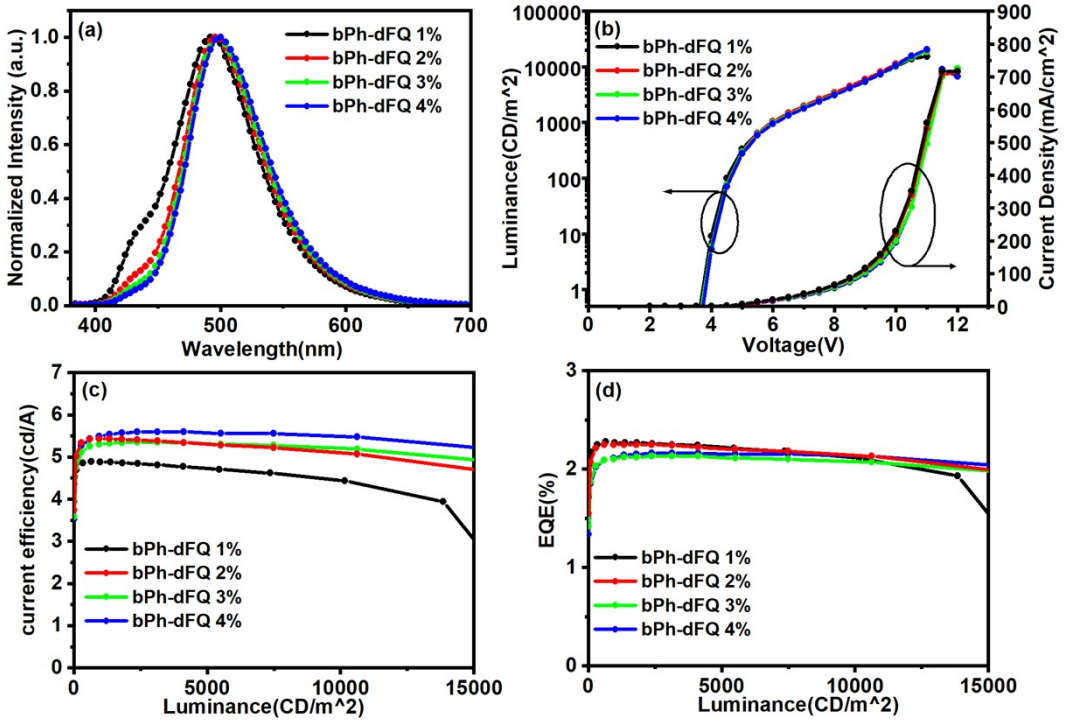

Figure S5.The EL performances of devices for compound bPh-dFQ as dopant concentration changed from 1% to 4%; (a) the EL spectrums at 8V for all the devices; (b) the current density–voltage-luminance (J-V-L) curves; (c) and (d) for the current efficiency and EQE vs luminance curves, respectively.

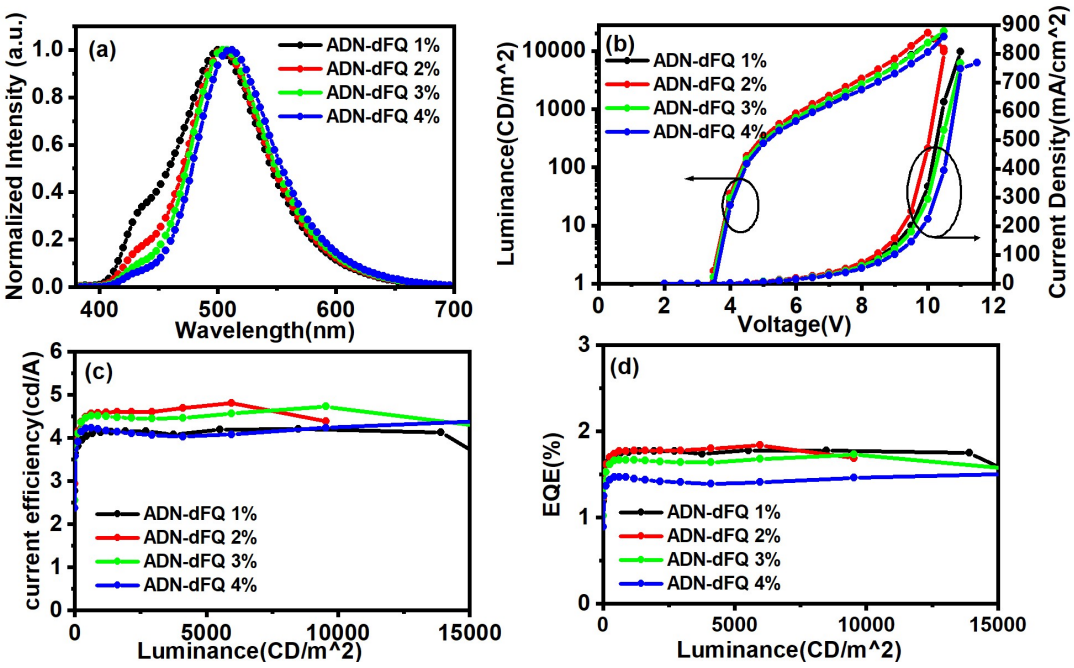

Figure S6. The EL performances of devices for compound ADN-dFQ as dopant concentration changed from 1% to 4%; (a) the EL spectrums at 8V for all the devices; (b) the current density–voltage-luminance (J-V-L) curves; (c) and (d) for the current efficiency and EQE vs luminance curves, respectively.

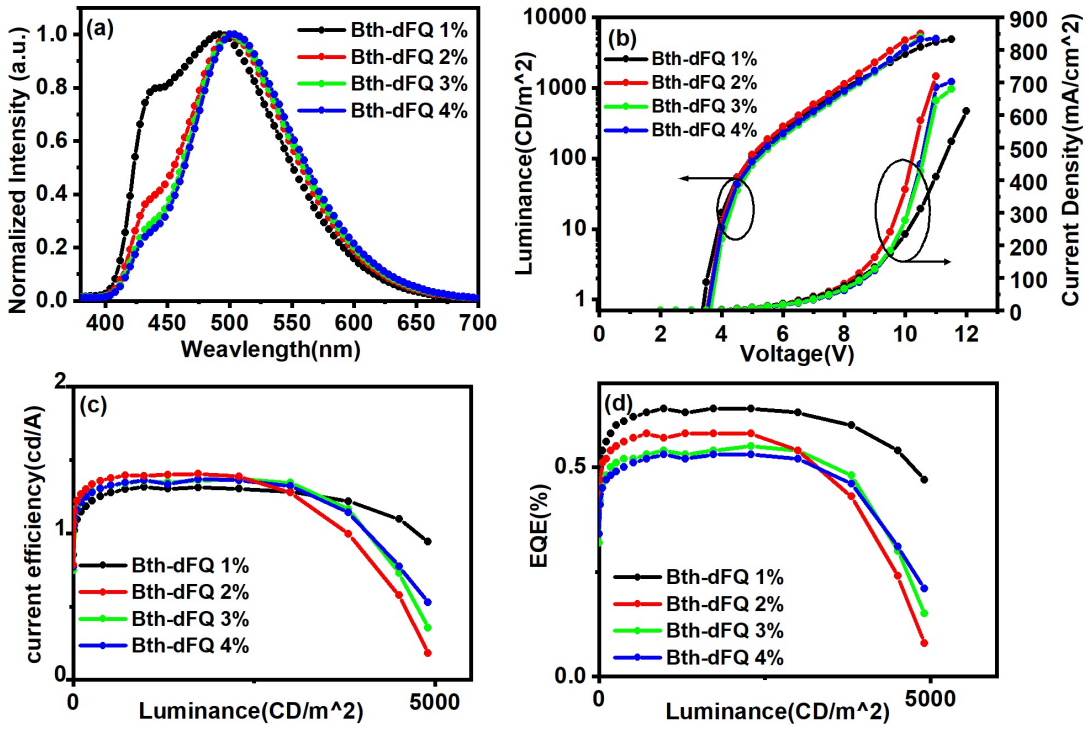

Figure S7. The EL performances of devices for compound Bth-dFQ as dopant concentration changed from 1% to 4%; (a) the EL spectrums at 8V for all the devices; (b) the current density–voltage-luminance (J-V-L) curves; (c) and (d) for the current efficiency and EQE vs luminance curves, respectively.

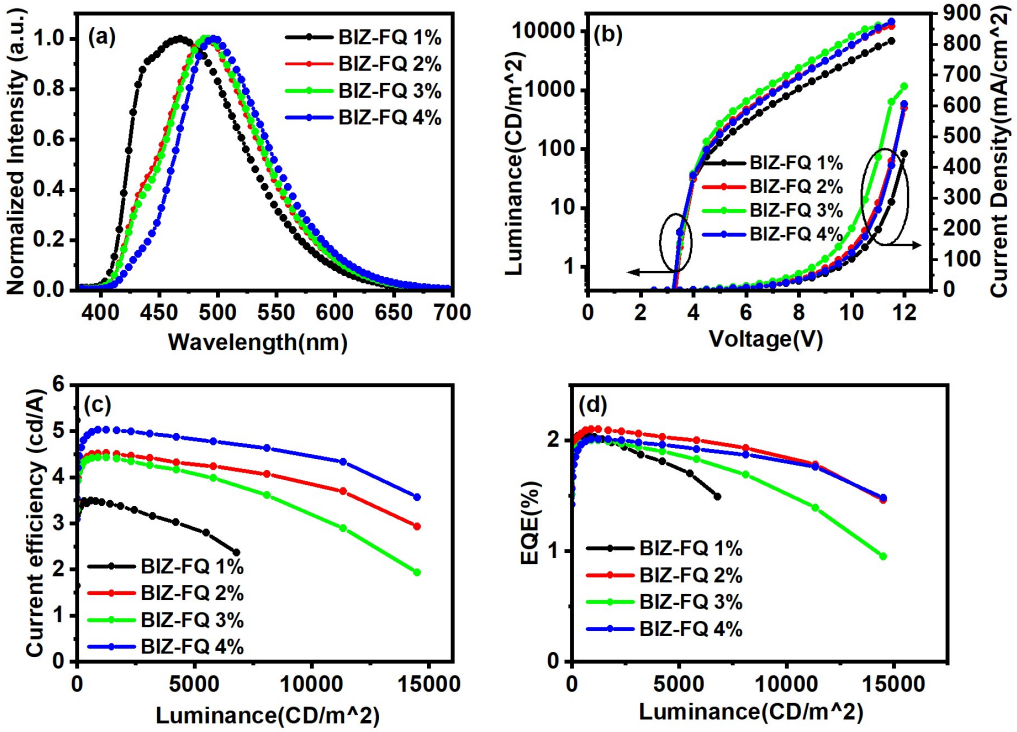

Figure S8. The EL performances of devices for compound BIZ-dFQ as dopant concentration changed from 1% to 4%; (a) the EL spectrums at 8V for all the devices; (b) the current density–voltage-luminance (J-V-L) curves; (c) and (d) for the current efficiency and EQE vs luminance curves, respectively.

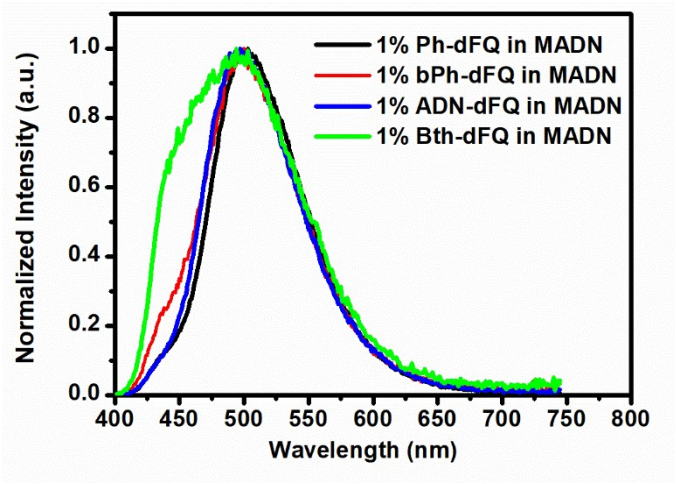

Figure S9 the PL spectra of 1% dopant (Ph-dFQ, bPh-dFQ ADN-dFQ, Bth-dFQ) doped MADN film

Section four: HNMR and HRMS spectra of five compounds

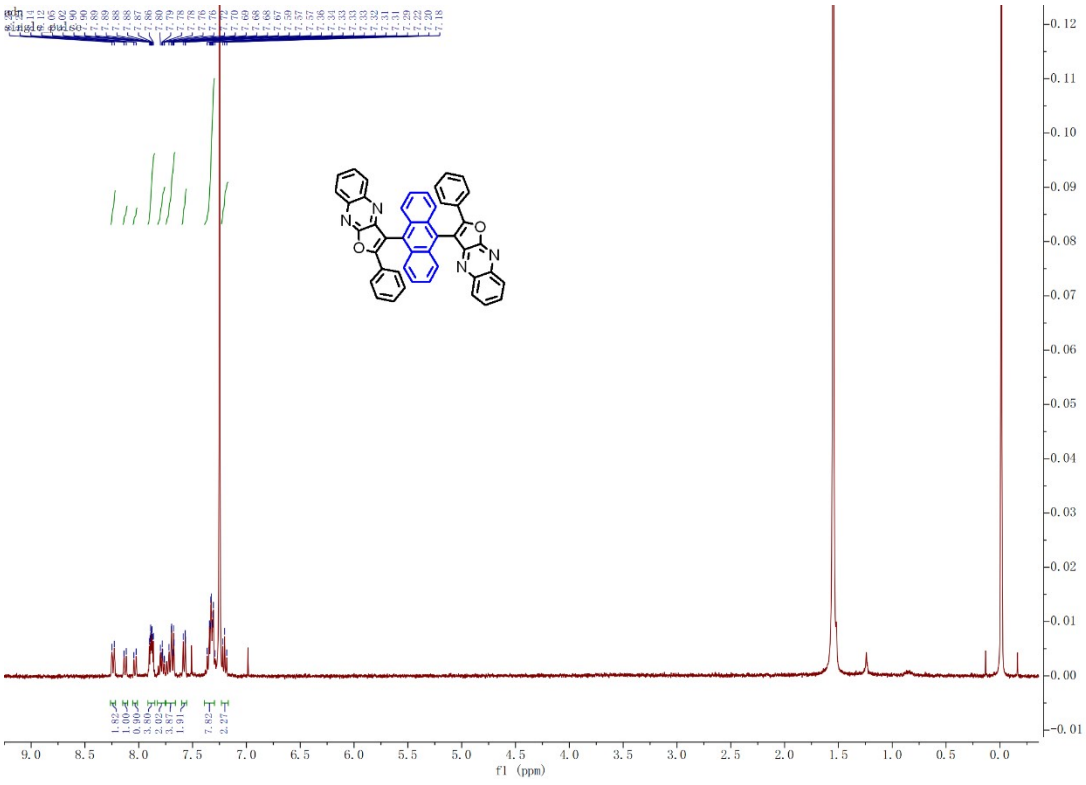

Figure S10 The ^{1}HNMR spectra of AND-dFQ

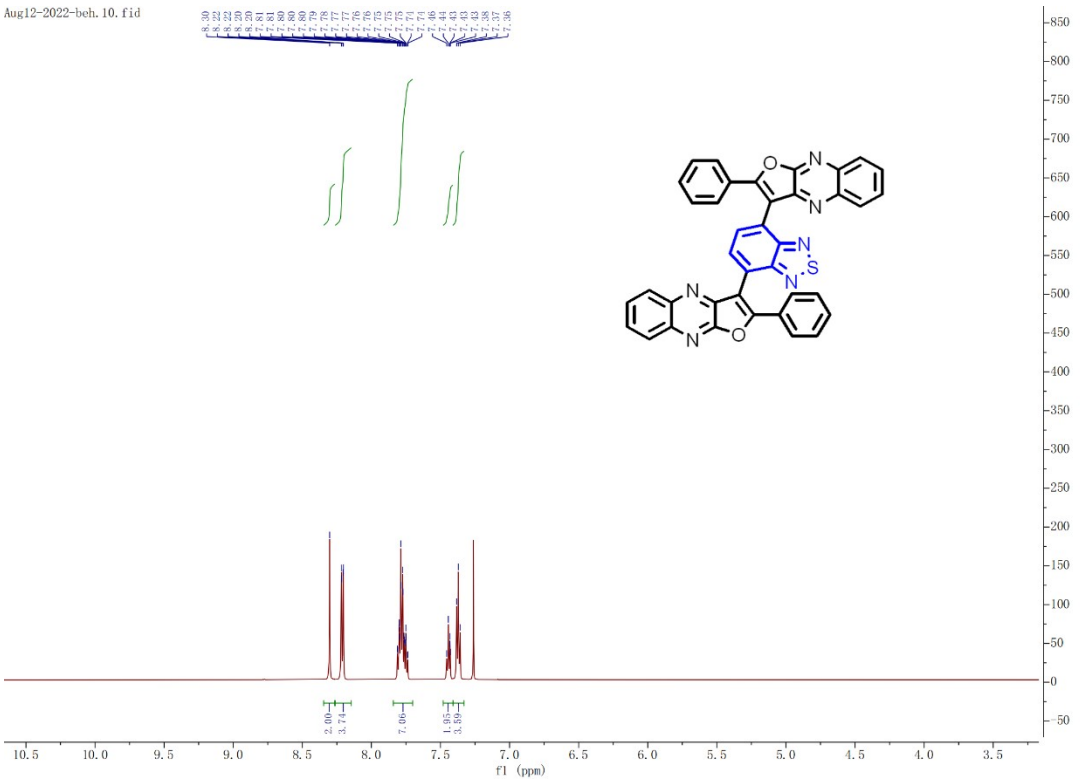

Figure S11 The ^{1}HNMR spectra of Bth-dFQ

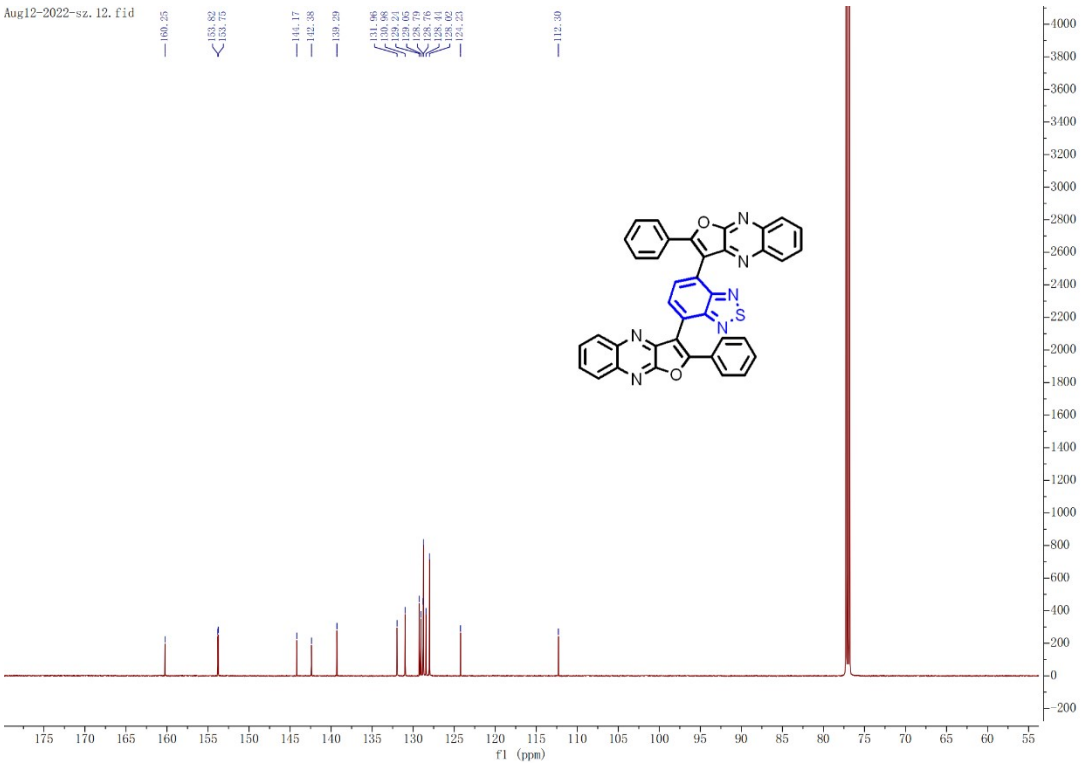

Figure S12 The ^{13}CNMR spectra of Bth-Dfq

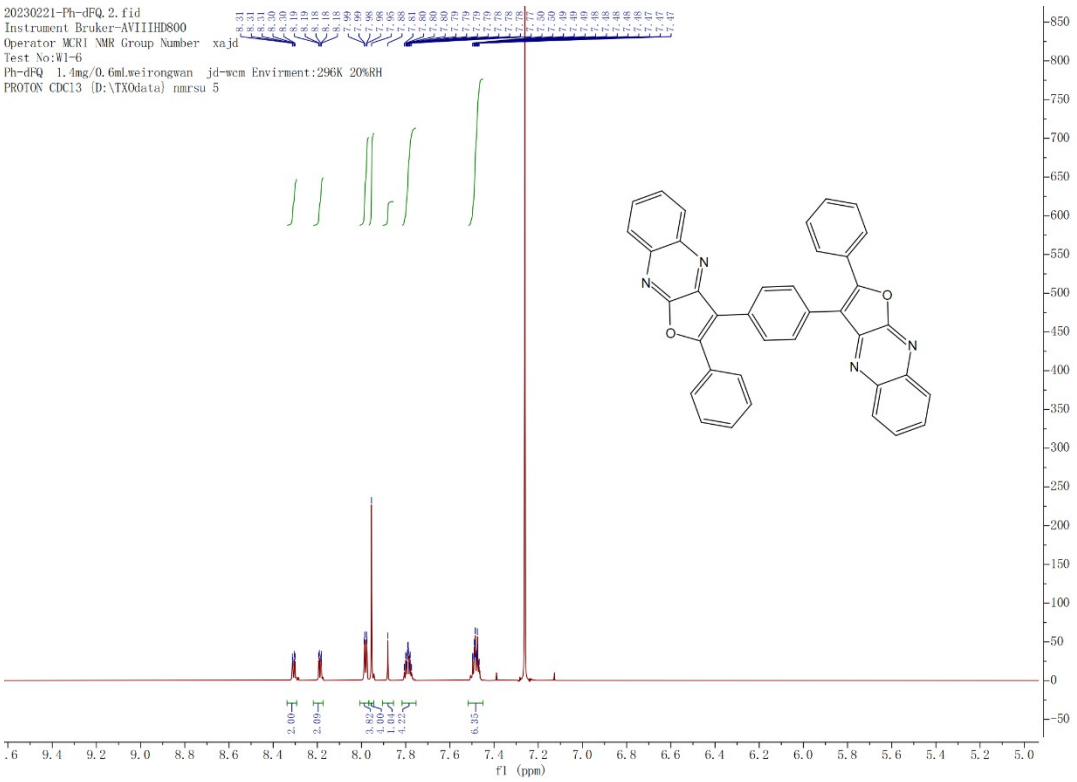

Figure S13 The ¹HNMR spectra of Ph-dFQ

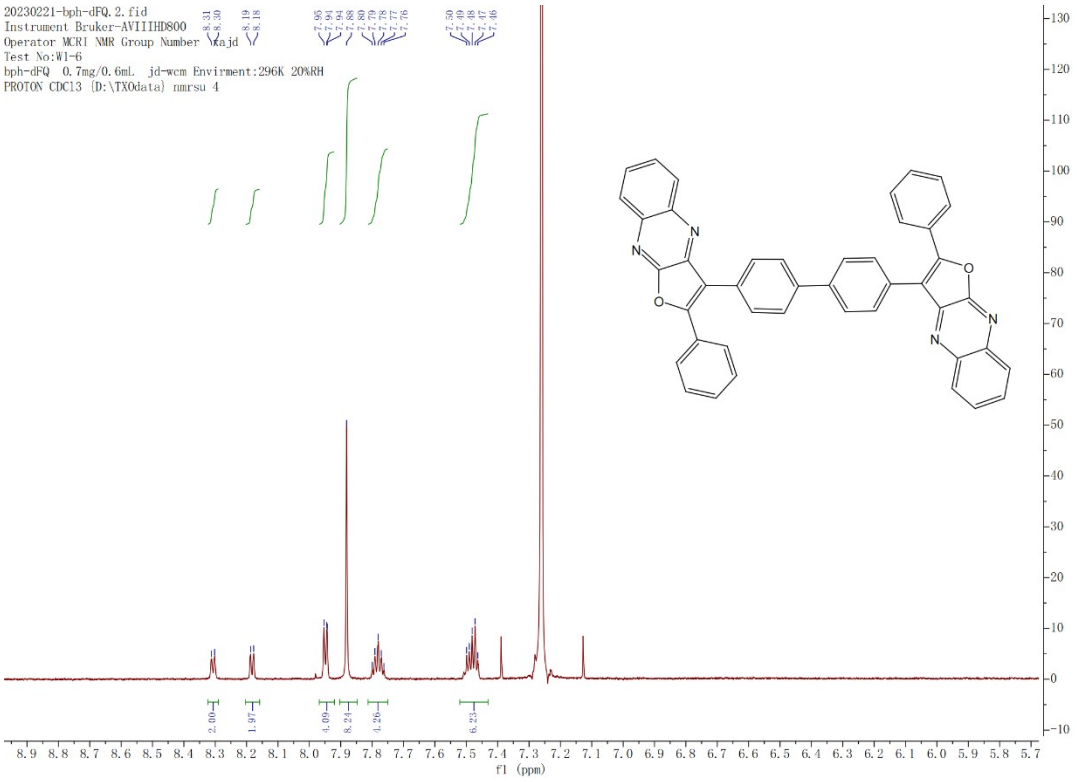

Figure S14 The ¹HNMR spectra of bPh-dFQ

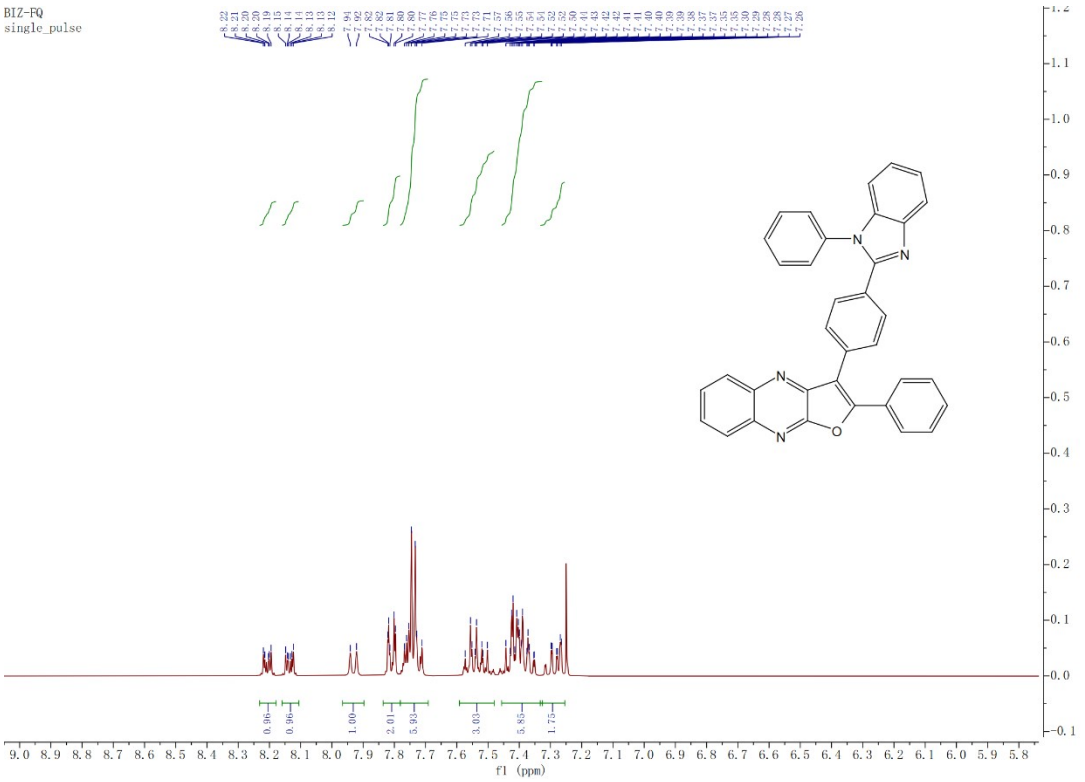

Figure S15 The ¹HNMR spectra of BIZ-FQ

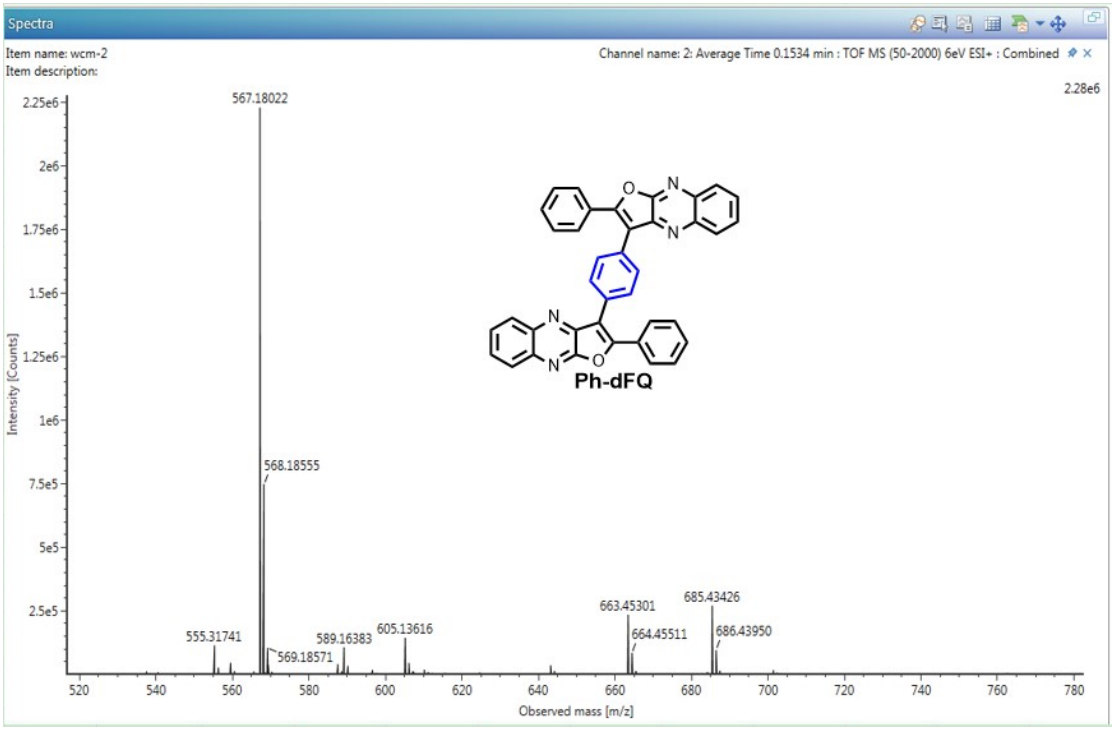

Figure S16 The HRMS spectra of Ph-dFQ

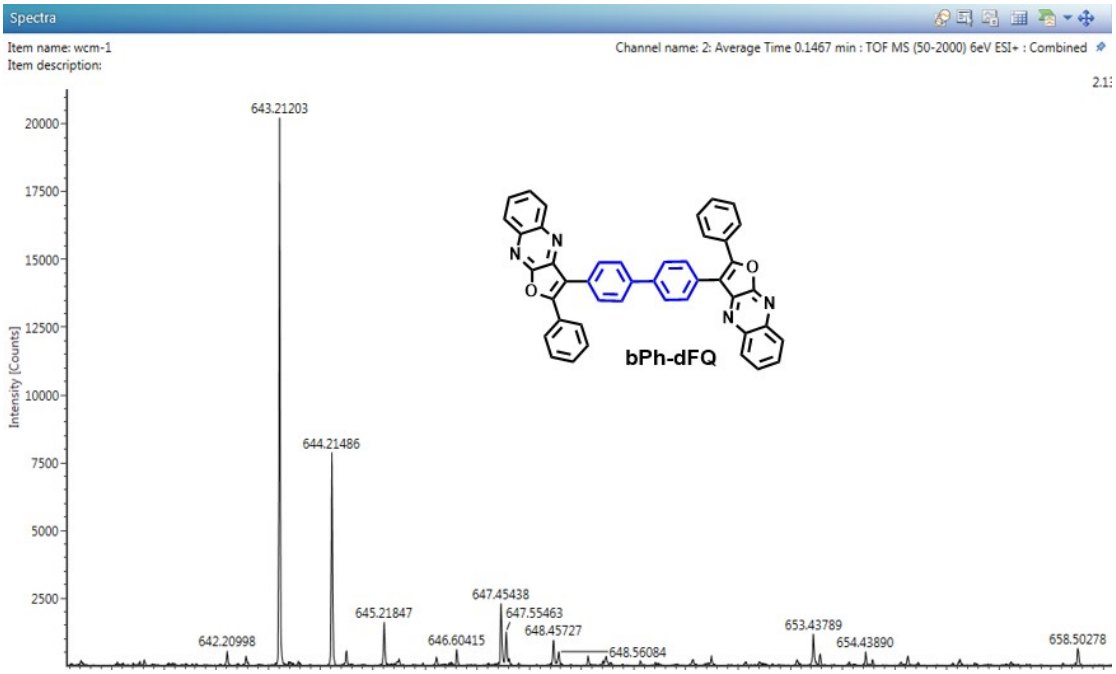

Figure S17 The HRMS spectra of bPh-dFQ

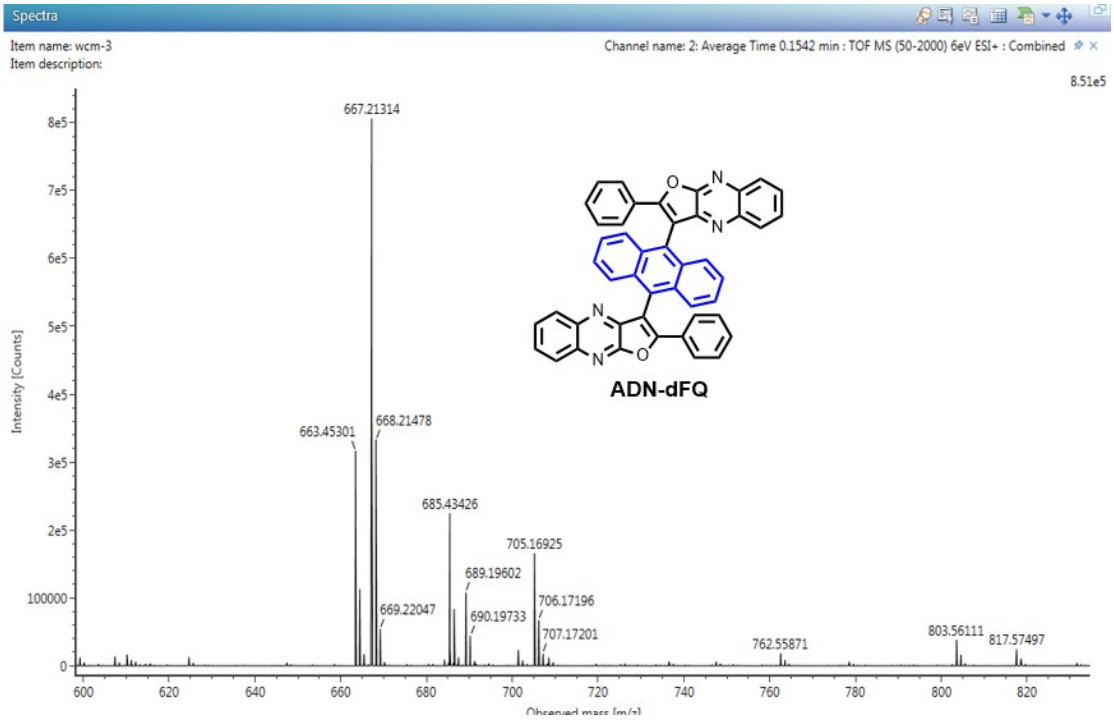

Figure S18 The HRMS spectra of ADN-dFQ

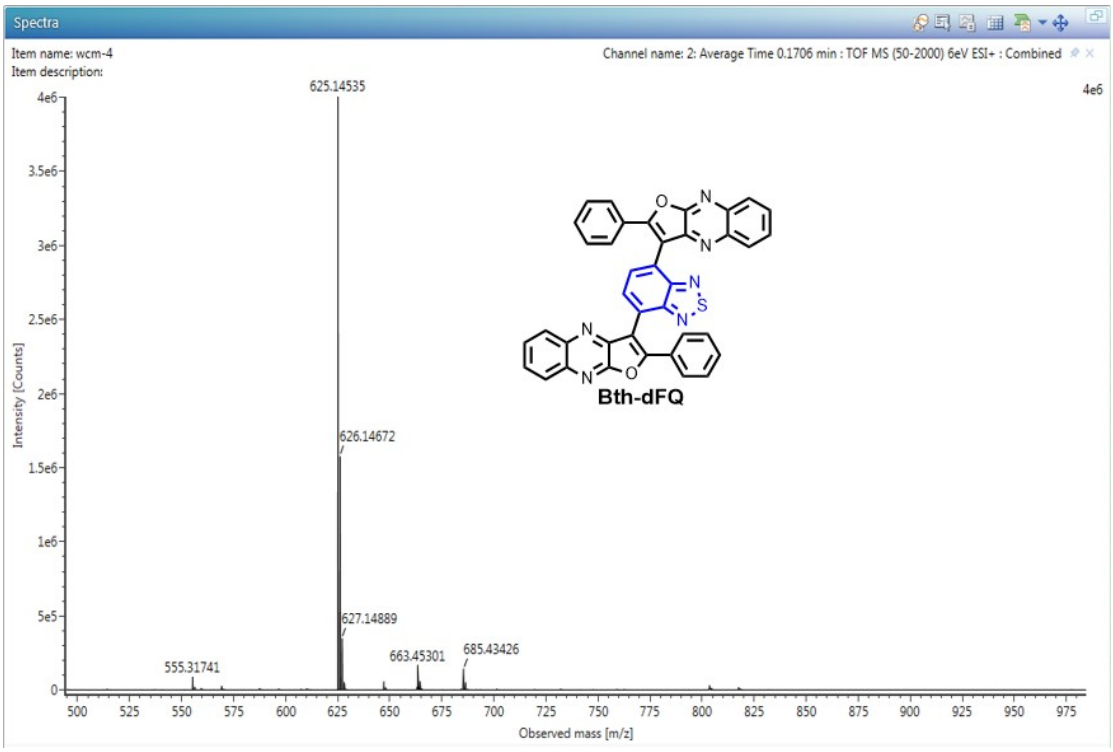

Figure S19 The HRMS spectra of Bth-dFQ

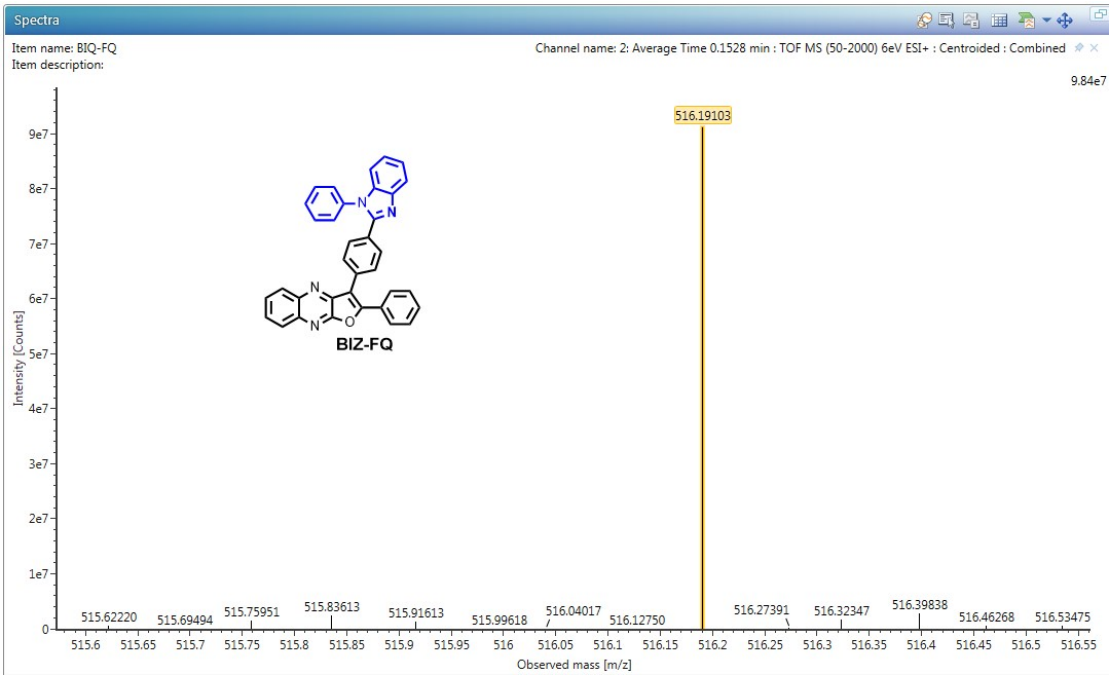

Figure S20 The HRMS spectra of BIZ-FQ